Automatic 3D City Reconstruction Platform Using a LIDAR and DGPS

Angel-Iván García-Moreno[1], José-Joel Gonzalez-Barbosa[1], Francisco-Javier Ornelas-Rodríguez[1], Juan-Bautista Hurtado-Ramos[1], Alfonso Ramirez-Pedraza[1], and Erick-Alejandro González-Barbosa[2]

[1] CICATA, Instituto Politécnico Nacional
Cerro Blanco 141 Col. Colinas del Cimatario, Quéretaro
jgonzalezba@ipn.mx
[2] Instituto Tecnolgico Superior de Irapuato-ITESI

Abstract. In this work an approach for geo-referenced 3D reconstruction of outdoor scenes using LIDAR (Light Detection And Ranging) and DGPS (Diferencial Global Positioning System) technologies is presented. We develop a computationally efficient method for 3D reconstruction of city-sized environments using both sensors providing an excellent base point for high-detail street views. In the proposed method, the translation between consecutive local maps is obtained using DGPS data and the rotation is obtained extracting correspondant planes of two point clouds and matching them, after extracting these parameters we merge many local scenes to obtain a global map. We validate the accuracy of the proposed method making a comparison between the reconstruction and real measures and plans of the scanned scene. The results show that the proposed system is a useful solution for 3D reconstruction of large scale city models.

Keywords: LIDAR, DGPS, 3D reconstruction.

1 Introduction

Terrestrial 3D laser scanning is a powerful tool for the surveyor. 3D laser scanning technology has become beneficial alternative in the collection of as-built data for manufacturing plant and facilities virtual reconstruction and management, as forest inventory characteristics such as vegetation height and volume as well as diameter at breast height. Other applications such as 3D modelling, as-built surveys, documentation, restoration and reconstruction of objects, require automatic processing of massive point clouds to extract surfaces of the recorded objects. In this work we introduces an approach for geo-registered 3D reconstruction of an outdoor scene using LIDAR technology and DGPS. We develop a computational method for 3D reconstruction of city-sized environments using both sensors providing a good base point for high-detail street views. Thus, remote sensing integrated with geospatial procedures and efficient field sampling techniques promises a fundamental data source for ecologically, socially and economically sustainable on-the-ground management.

I. Batyrshin and M. González Mendoza (Eds.): MICAI 2012, Part I, LNAI 7629, pp. 285–297, 2013.

The integration of aerial laser wiht GPS / IMU orientation systems has been widely used since the mid-90s because it provides good quality results and take advantage on a comprehensive manner of LIDARs airbone characteristics [14].

However, terrestrial lasers haven't followed the same path and are rarely directly targeted by a GPS / IMU. The integration of terrestrial laser with GPS / IMU sensors was carried out under project Geomobil [19] the mobile mapping system developed in ICC.

Using ground-based laser for tridimensional reconstruction of urban environments has grown considerably, the challenge is to create three-dimensional products with a minimal human intervention in processing information. Many laser scanning systems based on land vehicles have been developed in recent years [19] [9] [10] [12].

In [19] they use a Riegl laser $Z - 210$ capable of collecting up to $10,000$ points / second, intensity and RGB values are collected. The laser has a rotating mirror that allows taking vertical profiles while a servomotor rotates the system horizontally. All these raw data are parameters for a spherical coordinate frame. The GAMS (GPS Azimuth Measurement System) system allows to emulate differential GPS, in this case two antennas are mounted on the vehicle, the correction is made almost instantly achieving a data accuracy of 0.006 m.

Some other works incorporate an inertial measurement unit (IMU) and high precision GPS as in [9], also other sensors to generate high quality 3D views such as high resolution cameras for texturing point clouds [4], by using visual odometry algorithms (e.g. RANSAC or 7-point Hartleys algorithm [11]) they can determine the displacement and orientation of 3D point clouds although GPS are not sending information, this process is called Pose from Video (PfV).

In [12] merging data from different sensors (3 lasers, 2 high resolution cameras, 1 RTK GPS and inertial system) is given in real time, as they mounted the platform. The data of the video cameras are time tagged by the TERRAcontrol system which is synchronized with the laser scanner data. The TERRAcontrol computer gets the actual time from the global navigation satellite system (GNSS) receiver and distributes a time pulse together with a time stamp to the sensors. The accuracy GPS position in the kinematics conditions is 3 cm.

Most recently in [7]authors propose point cloud processing techniques to generate 3D maps from data captured by a system of detection and measurement through light. In this work, the authors presents two principal results: 2D maps for autonomous navigation and 3D maps reconstruction of urban scenes. This method is based on two techniques of segmentation of planes, the first one for a quick extraction of the main plane (the floor) and the second for the extraction of other planes (walls) [20].

2 Multisensorial Data Fusion

To provide our system with an acceptable quality and accuracy, We set up a multisensorial platform which is composed of a LIDAR laser sensor and a centimeter-precision GPS [1] [2]. While the laser sensor will provide the platform with three-dimensional data, the GPS will give for each laser acquisition its location into the world.

The used sensors are:

DGPS The GPS is a ProMark3 with RTK technology (Real Time Kinematic) single frequency and uses a double constellation for performance (GPS + SBAS) which allows GNSS surveys. The accuracy is variable and depends on the type of survey that we are doing, for real-time surveys have fixed RTK horizontal accuracy of 1 cm, post-processed static surveys collect data coordinates with an horizontal accuracy of 0.005 m, 0.01 m vertical and azimuth in arc second, on the other side kinematic works have an accuracy of 0.012 m horizontally, 0.015 m vertically.

LIDAR Velodyne© has developed and produced a High Definition LIDAR (HDL) sensor the HDL-64E, designed to satisfy the demands for autonomous vehicle navigation, stationary and mobile surveying, mapping, industrial use and other applications. The Velodyne HDL unit provides 360-degree azimuth field of view and 26.5-degree elevation field of view, up to 15 Hz frame refresh rate, and a rich point cloud populated at a rate of one million points per second. The HDL-64E operates on a rather simple premise: instead of a single laser firing through a rotating mirror, 64 lasers are mounted on upper and lower blocks of 32 lasers each and the entire unit spins. This design allows for 64 separate lasers to each fire thousands of times per second, providing exponentially more data points per second and a much richer point cloud than conventional designs. The HDL-64E is rated to provide usable returns up to 120 meters.

3 Urban Environments Digitalization Using LIDAR Technology

Our sensor array consisting in a differential GPS and a LIDAR mounted on a vehicle, connected to computer which is synchronized with the internal GPS clock to achieve a straight forward correlation of information from both sensors, as shown in Figure 1. Then using OpenGL libraries through primitive geometrics, in our case points, we are able to produce the 3D scenes by joining several acquisitions taken in different positions of the same capturing path.

3.1 Data Processing

After uprising, we end with gross data of the two sensors, we the process the data from the GPS and we assign these coordinates to the archives of the point clouds acquired by laser sensor. The procedure is done through the collation of the acquisition time between both sensors [15]. Seen otherwise its take the time of acquisition of a LIDAR file and look in the concentrate of the GPS coordinates and assigned to the file for further processing. Using the Cristian algorithm [6] we sync the time of two sensors.

Through `C++` developed program we attach the respective GPS coordinates to each point cloud. Sometimes the required time stamp is not in the database,

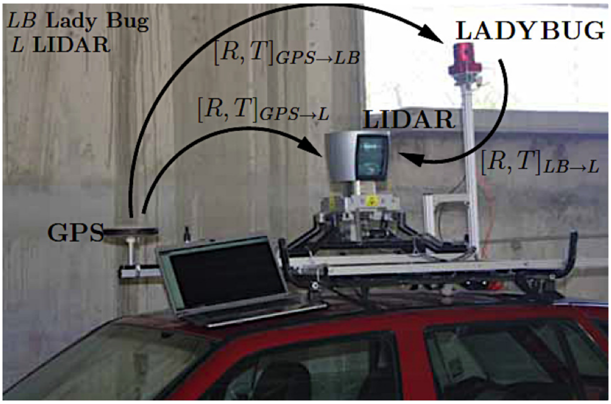

Fig. 1. Multisensor mobile platform

therefore we proceed to interpolate the positions that we do not have using a weighted interpolation:

$$\begin{aligned} \Delta_{gps} &= Gps_{n+1} - Gps_{n-1} \\ \Delta t_1 &= Gps_n - Gps_{n-1} \\ \Delta t_2 &= Gps_{n+1} - Gps_n \\ Missing\ Coordinate &= \frac{Coord_1 \ * \ t_1 \ - \ Coord_2 \ * \ t_2}{\Delta_{gps}} \end{aligned} \tag{1}$$

where Δ_{gps} is the weighting, Δt_1 y Δt_2 are the difference between the GPS acquisition time and missing time. This procedure is repeated for the longitude, latitude and elevation, which are independent data.

One of the algorithms used for data transformations from geographical coordinates to Euclidean coordinates, was the Coticchia - Surace algorithm [5]. The precision is one centimeter when using more than 5 decimals for all operations.

After coordinates are correlated with their respective acquisition of LIDAR sensor, we proceed to obtain the vectors of translation and rotation. Because the coordinates are in the UTM system, we obtain the translation vector with respect to a reference (x_0, y_0, z_0), this reference may be the position of an acquisition.

$$\underbrace{\begin{bmatrix} t_x \\ t_y \\ t_z \end{bmatrix}}_{\text{Translation vector}} = \begin{bmatrix} x - x_0 \\ y - y_0 \\ z - z_0 \end{bmatrix} \tag{2}$$

Where (x, y, z) denote the coordinates of the acquisitions, and (t_x, t_y, t_z) the translation vector between acquisitions and reference. So we get all translations for all acquisitions of the path to rebuild. To get the rotation first we define planes between two acquisitions and then rotate the second cloud on the first until matching the planes.

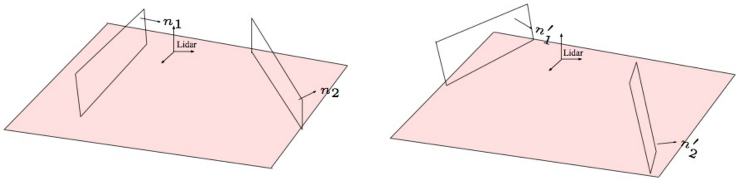

Fig. 2. Two acquisitions in different positions modeled by planes

Figure 2 shows two point clouds where their point of reference has been translated and rotated to match the environment planes. In [11], a plane referenced in two different coordinate systems is defined by the following equation:

$$\begin{bmatrix} n_i' \\ D' \end{bmatrix} = H^{-T} \begin{bmatrix} n_i \\ D \end{bmatrix} \tag{3}$$

Where $H = \begin{bmatrix} R & T \\ \mathbf{0}^T & 1 \end{bmatrix}$, R and T represents the rotation and translation matrix of 3×3 and 3×1 respectively. $\mathbf{0}$ denotes the null vector of 3×1. n_i and n_i' denote the normal unit vector of the planes referenced to the LIDAR coordinated system, which is not steady. D and D' denote the distance from the LIDAR point of reference to a plane in each point cloud. Therfore, the equation 3 is redefined as follows:

$$\begin{bmatrix} n_i' \\ D' \end{bmatrix} = \begin{bmatrix} R & \mathbf{0}^T \\ -(R * T)^T & 1 \end{bmatrix} \begin{bmatrix} n_i \\ D \end{bmatrix} \tag{4}$$

The resulting equations of two consecutive point clouds are used to calculate the rotation and translation between them. The equation 4 is redefined as:

$$F = \begin{bmatrix} n_i' \\ D' \end{bmatrix} - \begin{bmatrix} R & \mathbf{0}^T \\ -(R * T)^T & 1 \end{bmatrix} \begin{bmatrix} n_i \\ D \end{bmatrix} \tag{5}$$

R is given by Euler angles:

$$R = \begin{bmatrix} 1 & 0 & 0 \\ 0 & \cos(\theta_x) & -\sin(\theta_x) \\ 0 & \sin(\theta_x) & \cos(\theta_x) \end{bmatrix} \begin{bmatrix} \cos(\theta_y) & 0 & \sin(\theta_y) \\ 0 & 1 & 0 \\ -\sin(\theta_y) & 0 & \cos(\theta_y) \end{bmatrix} \begin{bmatrix} \cos(\theta_z) & -sin(\theta_z) & 0 \\ \sin(\theta_z) & \cos(\theta_z) & 0 \\ 0 & 0 & 1 \end{bmatrix}$$

The *Levenberg-Marquardt's* algorithm is used to compute the rotation and relation from the equation 5 and is given by:

$$\frac{\partial F}{\partial \Gamma} = 0\ ;$$

Where $\Gamma = \{\theta_x, \theta_y, \theta_z\}$.

3.2 Filtering

An inherent problem when working with lasers is the data acquisition noise, many factors such as environment, surface reflectance and the same sensor calibration are responsible for the digitization of an urban environment are noisy, that's why the information must be further processed to reduce this problem. The issue of filtering in 3D point clouds is fairly addressed in the state of art of the area [16] [13]. We used a version of principal component analysis (PCA) to maintain fine details without shrinking the data. The variant of PCA employed in this work makes a distribution of weights inversely proportional to the sum of the distances at which each data is from the average neighborhood ($V(p)$). Thus, more data are attacked far from the mean, so that outliers do not generate trend in this technique, we implemented the Eq. 6

$$W_i = \frac{1}{g_i \cdot \sum_{j=1}^{n} \frac{1}{g_i}} \tag{6}$$

Where W_i is the weight factor for each point, g_i is the average distance from each point of the neighborhood and n the number of neighborhood data. A weighted averange ($\bar{p}_w$) of the points was calculated with the equation 7, once having the points and the weighted averange og their neighborhood we placed them in the covariance matrix for to the PCA defined by Eq. 8.

$$\bar{p}_w = \frac{\sum W_i \, p_i}{\sum W_i} \tag{7}$$

$$MC_w = \frac{1}{n-1} \sum_{i=1}^{n} (p_1 - \bar{p}_w)(p_1 - \bar{p}_w)^t \, W \tag{8}$$

where $W = \left\{\sqrt{W_1}, ..., \sqrt{W_n}\right\}$ are the weights associated with each point p_i the neighborhood $V(p)$. After the envelope to prevent aliasing of the data was applied to a moving average of the points $\bar{p}$ in direction to normal of the tangent plane to $V(p)$. The normal n_m is calculated using the third eigenvector of the covariance matrix MC_w [8]:

$$\bar{p'}_w = \bar{p}_w + t_{min} \, n_m \tag{9}$$

where $\bar{p'}_w$ is the new mean position, $\bar{p}_w$ original mean, n_m is the normal to tangent plane of neighborhood in $\bar{p}_w$ and t_{min} is a displacement calculated by Eq. 10.

$$t_{min} = \sum_{p_i \in V(p)} n_w \, \|p_i - \bar{p}_w\| \tag{10}$$

4 Results

The previous sections described the three-dimensional reconstruction platform, a Lidar Velodyne and a differential GPS provide the system of necessary data to generate urban scenes. The LIDAR manufacturer specifies an accuracy of $\pm$ 5 cm in the collected data, however a home-made calibration of the scanner and the development of our own capture software allow us to obtain an accuracy of $\pm$ 1.6 cm [8]. Laser generates point clouds of local urban scenes that represent a portion of the total path, acquiring approximately a million points per second, these clouds are the ones we need to merge at the end of post-processing to generate global maps. At the same time, GPS records its position at a rate of one recording per second.

Our tests were carried out in the urban area close the research center in which work is developed, in Querétaro, México. We have chossen this place because it contains a variety of suitable of urban scenes, such as buildings, parking lots, shopping centers, areas without building, etc., which allow us to have an appropriate feedback appropriate all possible environments that form an area urbanized cities.

Geodesic points were acquired in the WGS84 (World Geodetic System 84) system because is a standard for mapping and has been also defined by the INEGI as standard in the Mexican Federation. In addition to allowing us to maintain the accuracy of the data to manage the information, either to interpolate the positions or switch from geodetic coordinates to flat through the conversion of spherical coordinates to flat through Coticchia-Surace algorithm could know the displacement and calculate the translation vector necessary to merge the local maps and generate the global view.

One of the major obstacles in this work was the computational performance, as shown in Figure 3 each of the marks indicate a capture position of the LIDAR sensor, if each of them is composed by around a million points, we are talking about a large amount of information to be processed, although the virtual 3D allocation of point clouds is not the problem, its manipulation is a big one, since the algorithms must be repeated thousands of times to generate the desired global scene.

In a parallel way to reduce the system works data, also would be eliminating of the maps much of sensor noise captures and the ground points, therefore to find appropriate distribution between time and distances of acquisition will provide our system with the speed and fidelity of data appropriate. Figure 4 shows three point clouds merged implementing the transformation algorithm Coticchia - Surace for obtaining the displacement, difference in acquisition times between each of them is 14 *second* at a speed of 40 km/h approximately . Notice the *blind spot* of the LIDAR in the center of the figure, also the considerable amount of information around this.

Merging several local acquisitons, our global map grows in vision depth, but obviously the final file size containing all data transferred also grows, in Figure 5 seen as being defined shapes and details merge grow as clouds, filtering these clouds, increase details because the noise of the clouds is decreased and shapes become more clear. Using a top view details are not seen properly, in Figure 6 can be seen at higher resolution the objects in the environment, a long trajectorie allows almost a complete rebuild of all objects, this is because data blocked in one local map can be obtenined in the next, or two or more cloud map later,

Fig. 3. LIDAR acquisitions

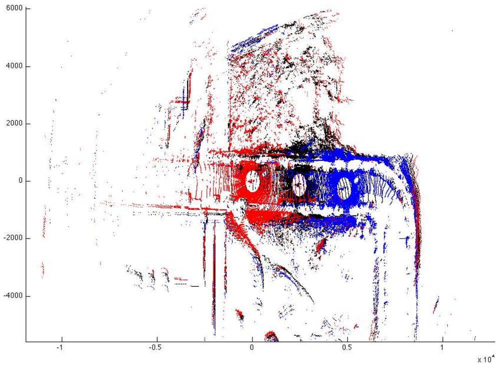

Fig. 4. Three merged data clouds, the displacement of the platform is left - right

mainly because the whole system is moving, allowing for multiple points of view of the same object. The previuos makes it possible to increase object definition and having a robust global map.

There are many other considerations in construction of global maps, for example in Figure 6, the material of certain objects tends to be relevant in the reconstruction, while dark colored objects absorb the laser intesity, light colors reflect almost the same intensity, and on the other hand, metallic objects tend to increase the intensity of the laser pulse and objects such as walls reduces the intensity, in this way the three-dimensional reconstruction with this technology denote implicitly these characteristics of the materials.

These results offer a clear perspective that terrestrial LIDAR technique is a viable option for the construction of three-dimensional urban scenes, where the external physical characteristics of the objects surface are not lost. We hope that by improving capture and fusion algorithms results can be also improved and, as a consequence precision can also be taken to better levels. As mentioned

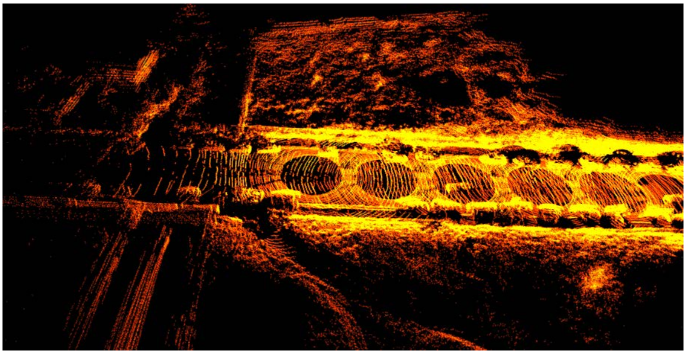

Fig. 5. Several local maps merged. The vision depth grows and objects resolution increase.

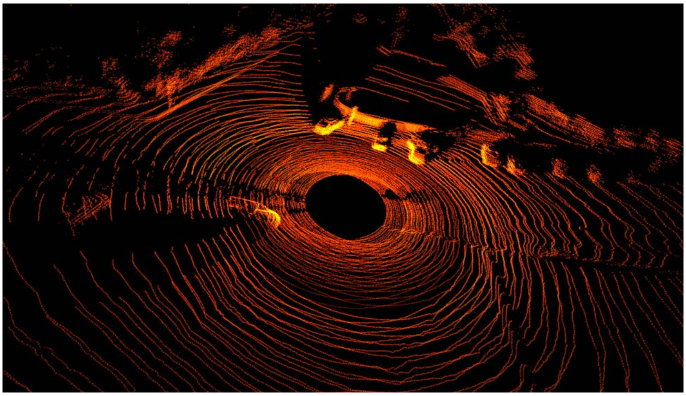

Fig. 6. Metal objects such as cars have higher reflectivity and perceived more defined

above, precision is now around 1.56 *cm* and its improvement will allow us for a closer-to-reality and more accurate global map.

4.1 Error Estimation Procedure

A controlled experiment was carried out using a closed-loop circuit in the shape of a parallelogram (Fig. 7). The idea of the path traced in this circuit is to have a good way for comparing results between our GPS dynamic acquisition and analysis system and reality. In addition a data filtering was carried out to basically erase all data referring the ground, which reduced the amount of procesed information.

It is important to know the error of our GPS system, to do so we used the closed-loop circuit as follows. We measured by hand the distances between each control point (see Fig. 7. Next we mounted the system on the vehicle and followed the circuit for a period of 30 minutes. Each control point (or *waypoint*)

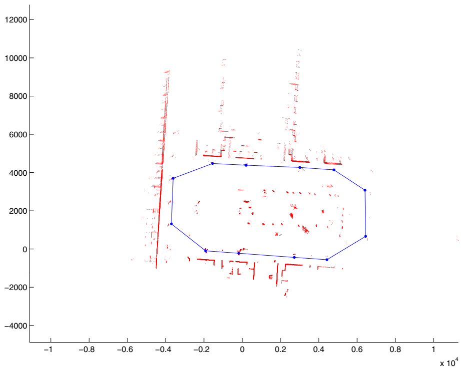

Fig. 7. Path control points for analysis accuracy

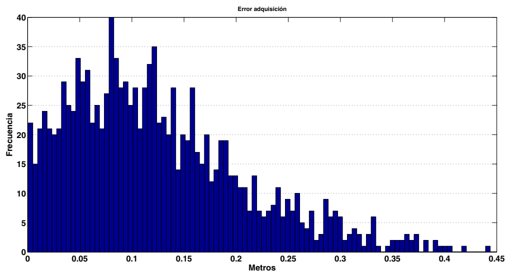

Fig. 8. Acquisition error, path vs. GPS data

location was acquired dynamically along the route. The final *waypoint* count was of around 2000 data points. Because the path described a parallelogram it was possible to obtain a set of equations describing each of its sides, notice that each line was defined by two consecutive *waypoints*. With this equations it was also possible to calculate the distances separating the *waypoints*. Finally, by comparing this calculated distances with those taken by hand (assuming the lasts were true) we were able of obtaining a good estimation of the average error in the dynamic capturing system. The average error ranged from 0 to 50 cm which we considered quite acceptable given the capture conditions (our capturing system is always in motion). See for example [18] and [3] where a traslation error of 30 and 12 cm was obtained with a static system.

Once a set of individual point clouds has been merged, error of fused data is also estimated. This estimation is necessary because the acquisition methodology induces a cumulative error from one capture to the next. By using a closed-path it is ensured that some objects and surfaces are captured in all or several 3D scenes, using this objects as references an error evaluation is possible. Error estimation procedure is described next. We started with the definition of some specific straight lines belonging to some walls, not all the lines but only those visible from an aerial view (we called them reference lines) as they will be seen in an architectural plane, to create this reference lines we made a line fitting of all points defining a wall used as reference. The fitting is needed because the Lydar has an intrinsic error an not all points assigned to a flat object lie in the same plane. The next step is to trace a perpendicular line to each of the reference lines, this perpendicular must also pass through a reference point (those points on parallelogram vertices). Finally we compare the perpendicular position resulting from one capture to the perpendicular position of a different capture. Remember that we have obtained multiple captures by doing the same path several times. After comparison we are in the position of obtaining a good estimation of the cumulative error induced in our readings due to the error on GPS positioning. Cumulative error is shown in Fig. 9 and 10 were one can see that the error is bigger towards the end of the loop.

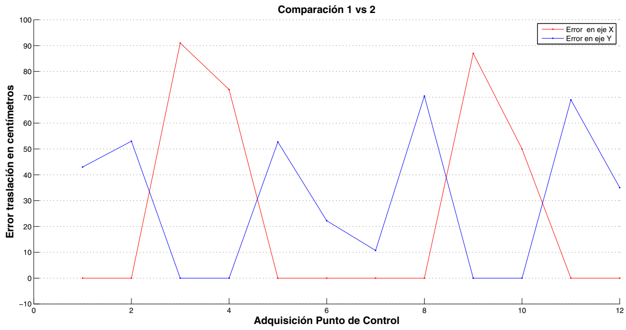

Fig. 9. Accumulated error between the first and second acquisition in the control circuit

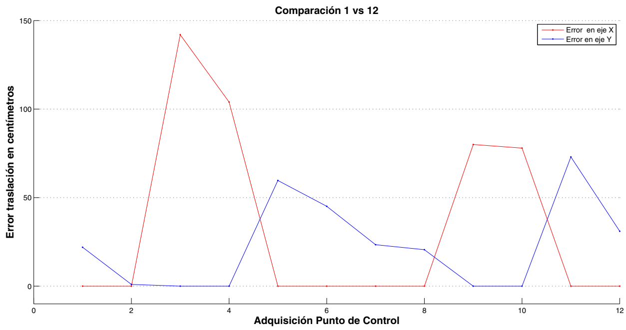

Fig. 10. Accumulated error between the first and last acquisition, completed loop

5 Conclusions and Future Work

An automatic 3D building system requires the least extra effort by users and the equipment used during the procurement field. The accuracy of the information processing should be the most optimal, but now with terrestrial systems, 3D reconstruction is rarely enough by many factors such as noise, viewing angles, speed of which is mounted mobile platform acquisition and performance of the hardware used.

We have presented experimental results of 3D city construction of a system consisting of a Velodyne LIDAR 64E and a differential GPS. Our system can acquire data for several kilometers in real time and fast processing of information to generate accurate three-dimensional scenes.

Among the additional work presented in this paper are debugging and generate georeferencing algorithms and interpolation of data faster and robust, as well as conversion to other flat coordinates by more elaborate processes [17]. Improving the quality of global scenes generated by a most complete calibration of the sensors and improve the automation of data processing tasks. We plan to implement a 3D SLAM algorithm. It is also in our plan to extend partially the Orthogonality to outdoor city-like environments where the constraint of vertical planes holds for most buildings. Alternate work this would complement the view of the scene, as the segmentation of objects not belonging to the environment and the texturing of the point cloud.

Commonly used methods in this field depend of video elements and photogrammetric that provides accurate works but with long time post-processing, that is why the integration of our system will drastically reduce the time to obtain efficient 3D scene point clouds to obtain quickly and a low cost of operation.

This demonstrates that a terrestrial technique for a LIDAR technology can be considered a new alternative rather than traditional methods such as LIDAR and aerial photogrammetry for three-dimensional reconstruction of urban environments.

References

1. Amoureus, L., Bomers, M.P.H., Fuser, R., Tosatto, M.: Integration of lidar and terrestrial mobile mapping technology for the creation of a comprehensive road cadastre. In: The 5th International Symposium on Mobile Mapping Technology, pp. 29–31 (2007)
2. Böhm, J., Haala, N.: Efficient integration of aerial and terrestrial laser data for virtual city modeling uusing lasermaps. Proceedings of the ISPRS Workshop, Laser scanning (2007)
3. Bok, Y., Hwang, Y., Kweon, I.S.: Accurate motion estimation and high-precision 3d reconstruction by sensor fusion. In: Optimization, pp. 4721–4726 (April 2007)
4. Chen, L.C., Teo, T.A., Rau, J.Y., Liu, J.K., Hsu, W.C.: Building reconstruction from lidar data and aerial imagery. In: International Geoscience and Remote Sensing Symposium, vol. 4, pp. 2846–2849. IEEE (2005)
5. Coticchia, A., Surace, L.: La trasformazione delle cordinate dal sistema UTM. Laboratorio di Topografia e Fotogrammetria (1984)

6. Cristian, F.: Probabilistic clock synchronization. Distributed Computing, 146–158 (1989)
7. de Jesus Rico-Jiménez, J.: Construcción de mapas 3d a partir de la extracción de primitivas geométricas obtenidas de datos de un lidar. Tesis de Maestría (2009)
8. González-Barbosa, J.-J., Atanacio-Jiménez, G., et al.: Lidar velodyne hdl-64e calibration using pattern planes. International Journal of Advanced Robotics Systems (2011)
9. Grinstead, B., Koschan, D.: Vehicle-borne scanning for detailed 3d terrain model generation. In: SAE Commercial Vehicle Engineering Congress (2005)
10. Haala, N., Peter, M.: Mobile lidar mapping for 3d point cloud collection in urban areas - a performance test. In: 21 ISPRS Congress (2008)
11. Hartley, R., Zisserman: Multiple view geometry in computer vision. Cambridge University Press (2000)
12. Kremer, J., Hunter, G.: Performance of the streetmapper mobile lidar mapping system in ”real world” projects. Photogrammetric Week (2007)
13. Leal, E., Leal, N.: Point cloud denoising using robust principal component analysis. In: International Conference on Computer Graphics Theory and Applications, pp. 51–58 (2006)
14. Lindenberger, J.: Laser-Profilmessung zur topographischen Geländeaufnahme. PhD thesis, Deutsche Geodätische Kommission bei der Bayerischen Akademie der Wissenschaften (1993)
15. Mettenleiter, M., Obertreiber, N., Härtl, F., Ehm, M., Baur, J., Fröhlich, C.: 3d laser scanner as part of kinematic measurement systems. In: 1st International Conference on Machine Control and Guidance, pp. 24–26 (2008)
16. Mitra, N.J., Nguyen, A., Guibas, L.: Estimating surface normals in noisy point cloud data. Special Issue of International Journal of Computational Geometry and Applications 14, 261–276 (2004)
17. Snyder, P.: Usgs no. 1532. Map Projections used by the United States Geological Survey
18. Sprickerhof, J., Lingemann, K., Hertzberg, J.: A heuristic loop closing technique for large-scale 6d slam. Automatika, 199–222 (2011)
19. Talaya, J., Bosch, E.: Geomòbil: the mobile mapping system from the icc. In: 4th International Symposium on Mobile Mapping Technology (2004)
20. Verma, V., Kumar, R., Hsu, S.: 3d building detection and modeling from aerial lidar data. In: 2006 IEEE Computer Society Conference on Computer Vision and Pattern Recognition, vol. 2, pp. 2213–2220. IEEE (2006)